Variability modes and typical patterns of surface wind over the Japan/East Sea and adjacent land

O. Trusenkova[1], S. Stanichny[2], and Yu. Ratner[2]

[1]V.I. Il'ichev Pacific Oceanological Institute, Vladivostok, Russia
[2] Marine Hydrophysical Institute, National Academy of Sciences of Ukraine

Background

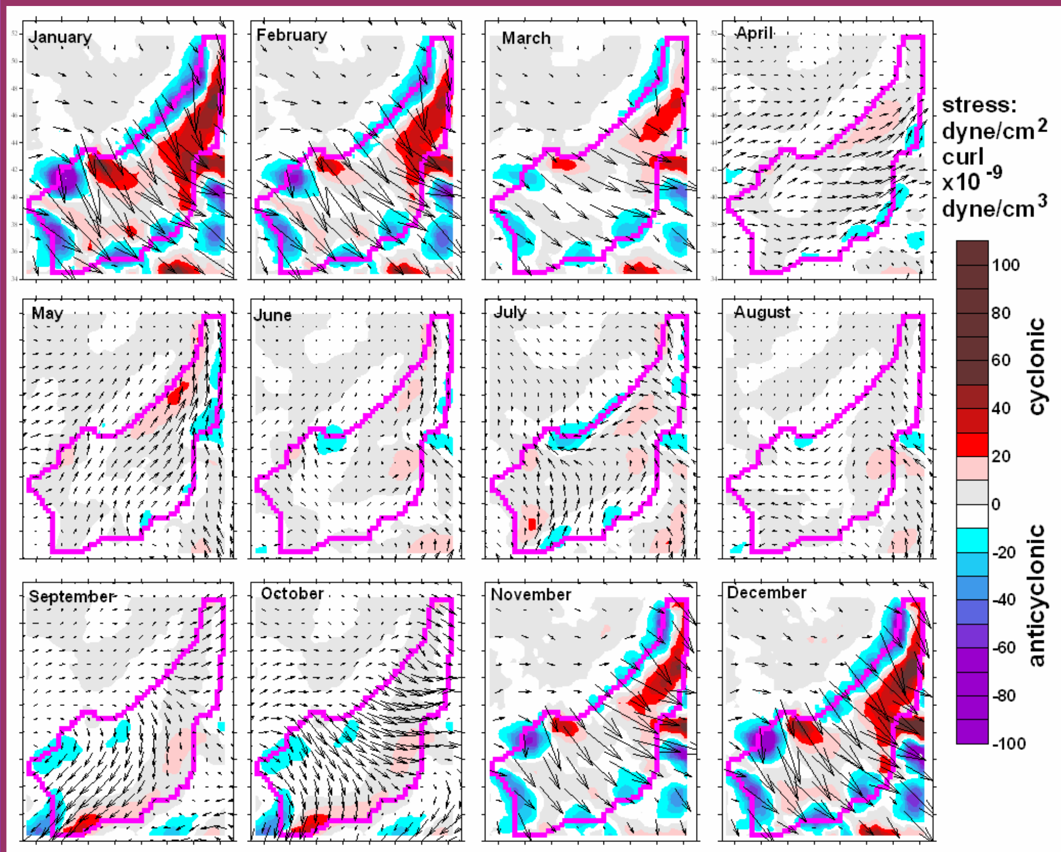

Wind stress and curl 1998-2005 NCEP/NCAR

Effect of winter wind stress and curl (Yoon et al., 2005)

Impact of summer wind (Trusenkova et al., 2005) and unsatisfactory monthly mean winds for the summer monsoon

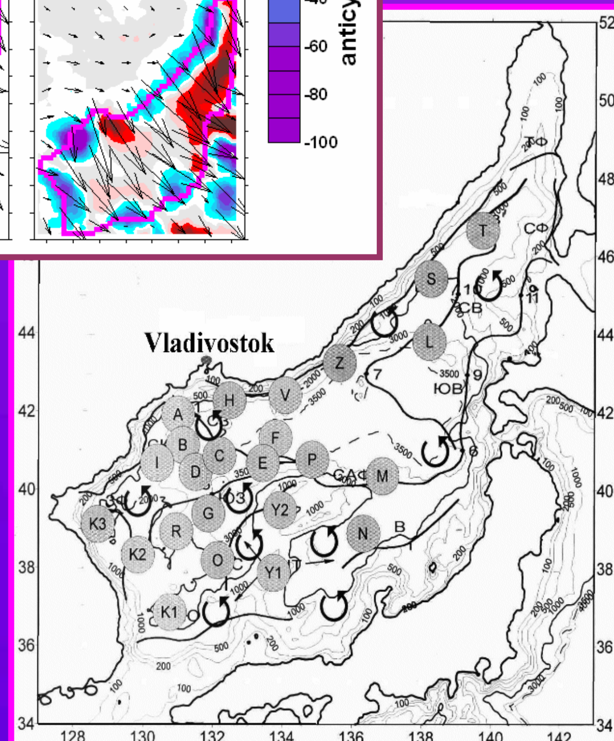

Eddies in the JES (Nikitin, 2006)

Extremely high mesoscale and interannual variability

Purpose of the study

- To reveal major variability modes of surface wind over the JES and adjacent land
- To obtain typical wind patterns and estimate their intra- and interannual variability
- To demonstrate features of the JES circulation induced by the wind stress and curl patterns

Data

NCEP/NCAR 4 times daily

1°x1°-gridded wind for 1998-2005
(SeaWiFS Project Ancillary Data)

34°-53°N, 127°-143°E
(JES and adjacent land)

- Throughout wind stress dataset for the whole period (11580 fields)
- Wind stress datasets for every month (904 to 992 fields)

Complex Empirical Orthogonal Function (CEOF) Analysis

(Decomposition to Complex Normal Modes)

$\mathbf{X}(\mathbf{r}, t) = \sum A_k(\mathbf{r})B_k(t)$,

where

$\mathbf{X}(\mathbf{r}, t) = U(\mathbf{r}, t) + iV(r, t)$ is initial complex signal, with zonal/meridional wind constituting its real/imaginary parts,

$A_k(\mathbf{r}) = \mathit{A}_k(\mathbf{r})e^{-i\varphi}$ are spatial CEOFs,

$B_k(t) = \mathit{B}_k(t)e^{-i\phi}$ are principal components (PCs),

A_k, B_k are spatial and temporal amplitudes, respectively;

they determining the mode intensity,

φ_k, ϕ_k are spatial and temporal phases

defined from от $-\pi$ (-180°) to π (180°);

they determine wind shear in space and time, respectively.

CEOF1-CEOF3
Spatial amplutudes/phases

Whole year | January | April (~September) | July

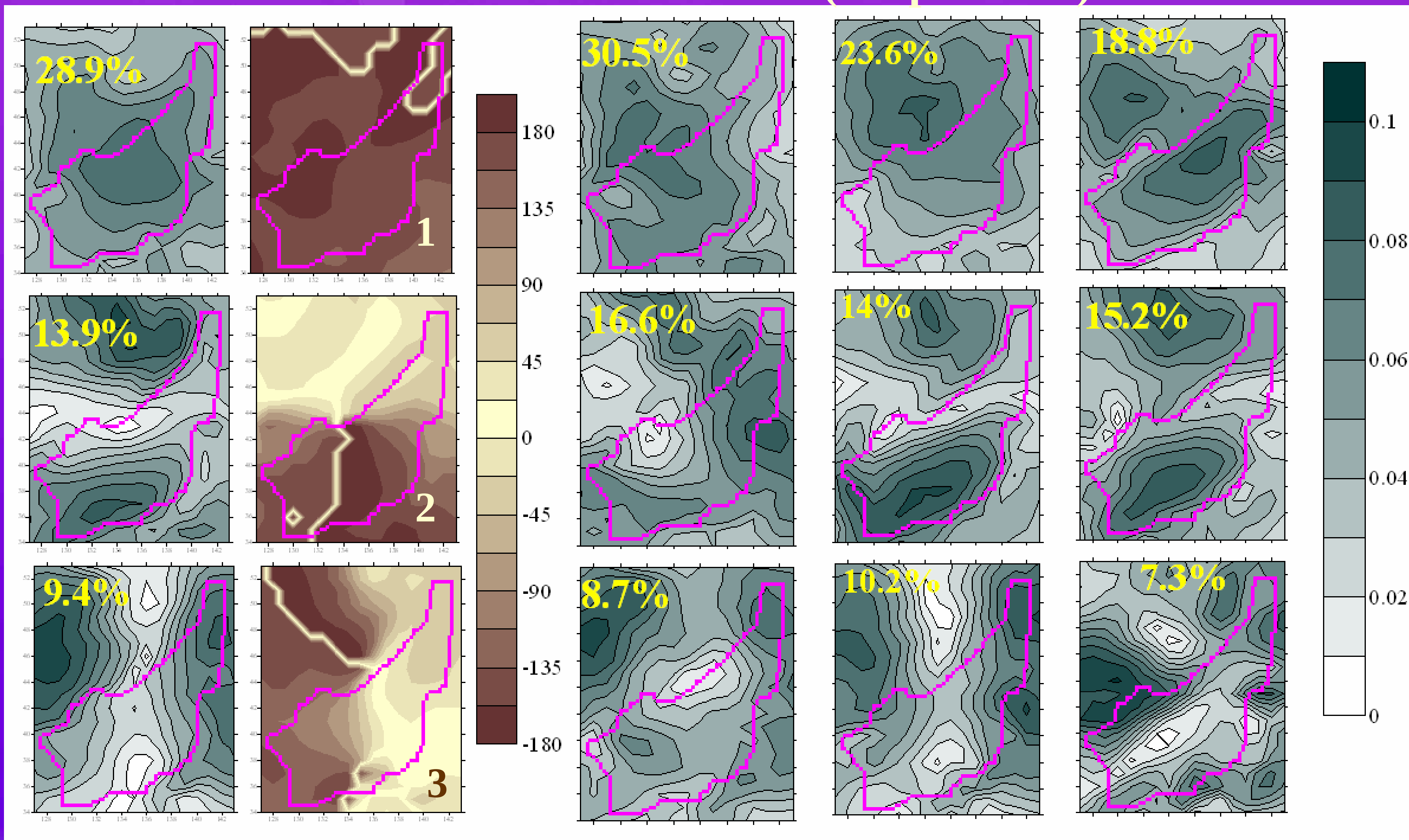

PC1-PC3
Temporal amplutudes/phases

Whole year

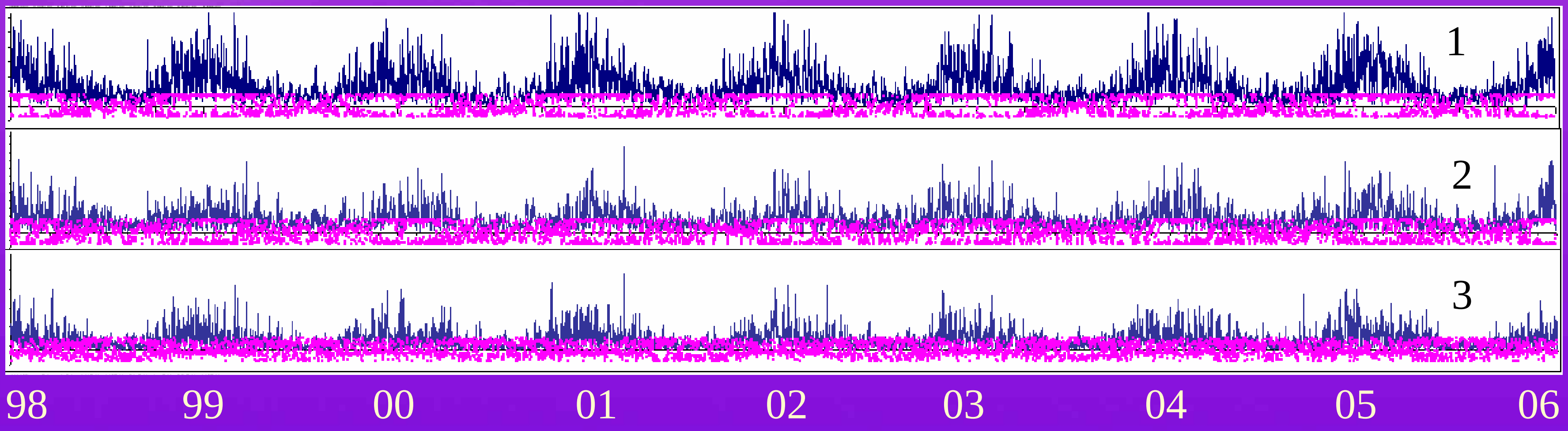

January

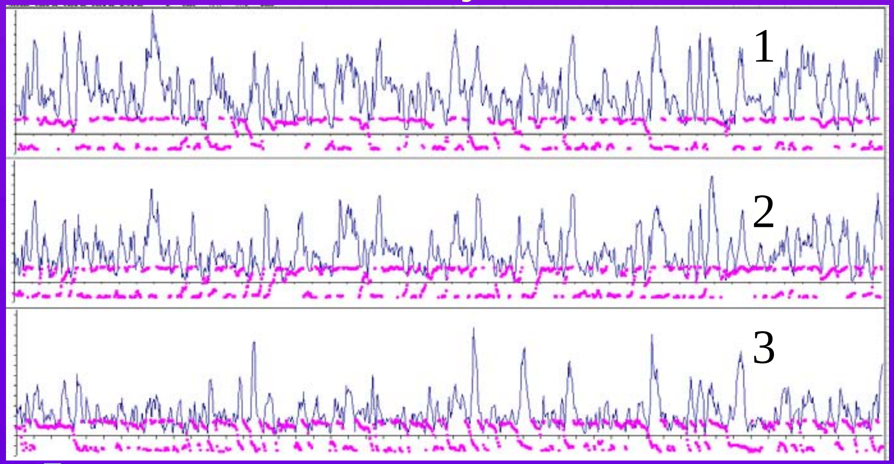

July

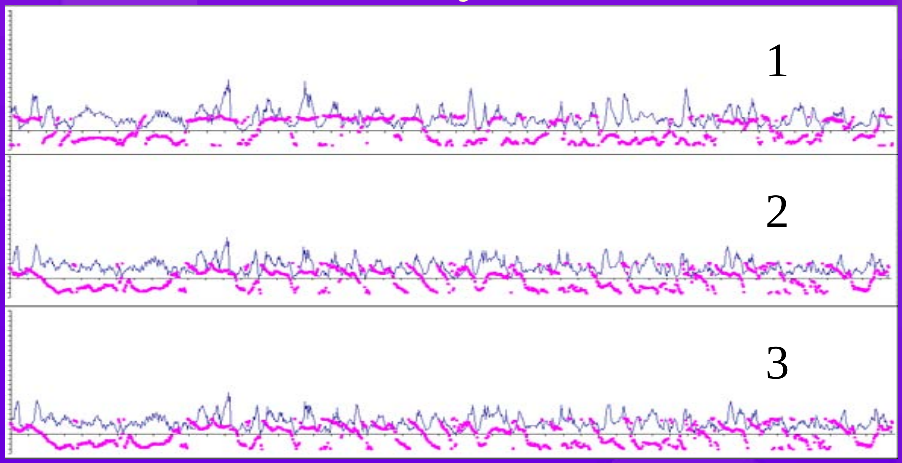

Amplitude (dyne/cm^2) in blue, phase (rad) in magenta

PC1-PC3 phase intervals for October

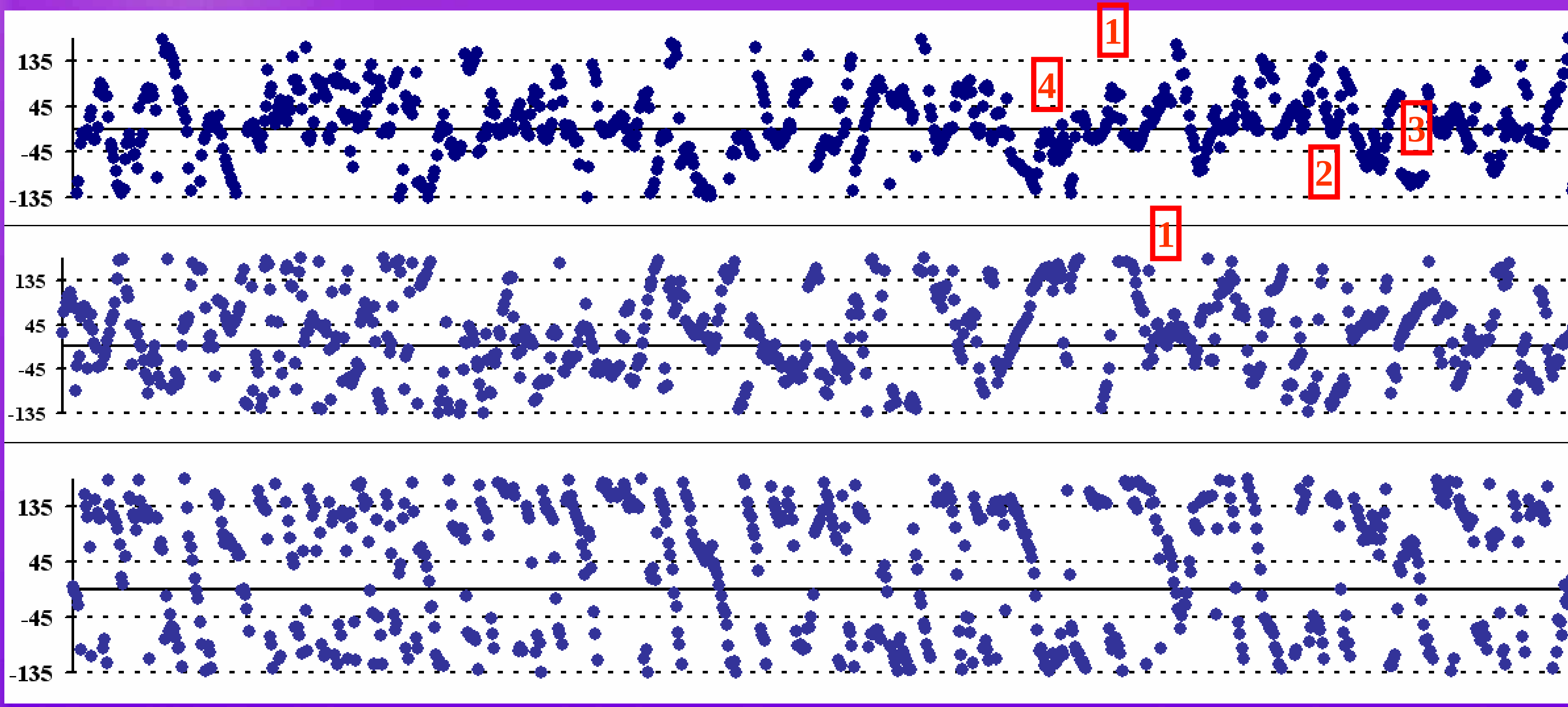

Number of classes:
$n = 2\pi/\Delta\varphi$, where
$\Delta\varphi$ is temporal phase interval

(Trusenkova et al., 2006)

Class 1: $\varphi < -3\pi/4 \cup \varphi > 3\pi/4$
Class 2: $-3\pi/4 < \varphi < -\pi/4$
Class 3: $-\pi/4 < \varphi < \pi/4$
Class 4: $\pi/4 < \varphi < 3\pi/4$

Major variability modes

For the whole year

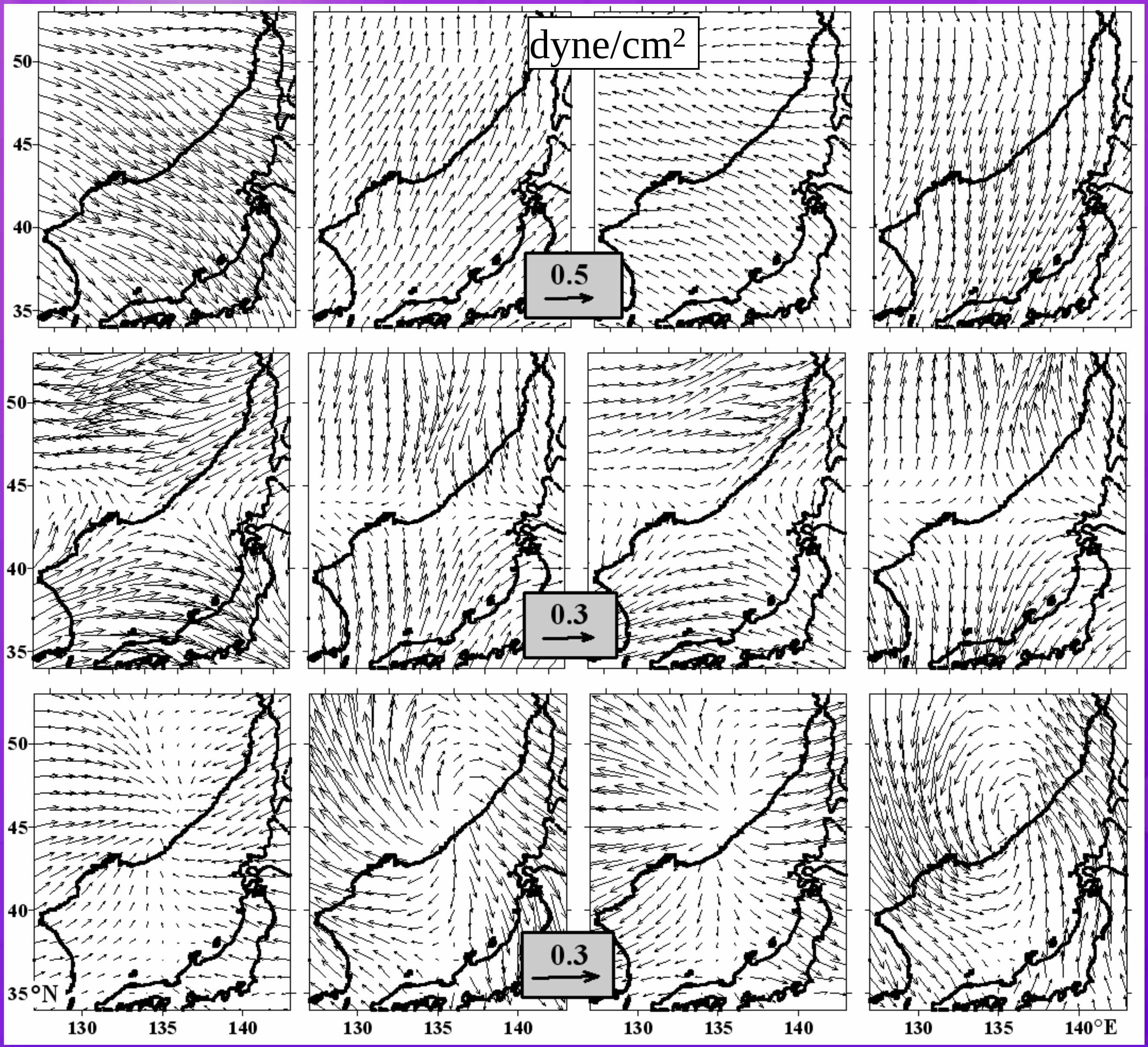

CEOF1: 42%, 25%, 15%, 18%

CEOF2: 33%, 21%, 24%, 22%

CEOF3: 10%, 36%, 24%, 30%

EOF analysis of ECMWF winter zonal & meridional wind (Dashko and Varlamov, 2000)

Typical wind patterns

Method of construction:

CEOF decomposition of monthly datasets

↓

Classification of initial fields by PC1 temporal phase for every month (6 to 8 classes)

↓

Typical wind patterns with prevailing wind direction as average fields for the classes

Good agreement with

Glebova (1998): expert classification of 10-day-mean SLP fileds, with the use of circulation Kats indices

Prevailing wind direction as the *classifying attribute*

Northwest (NW) and northern (N) patterns

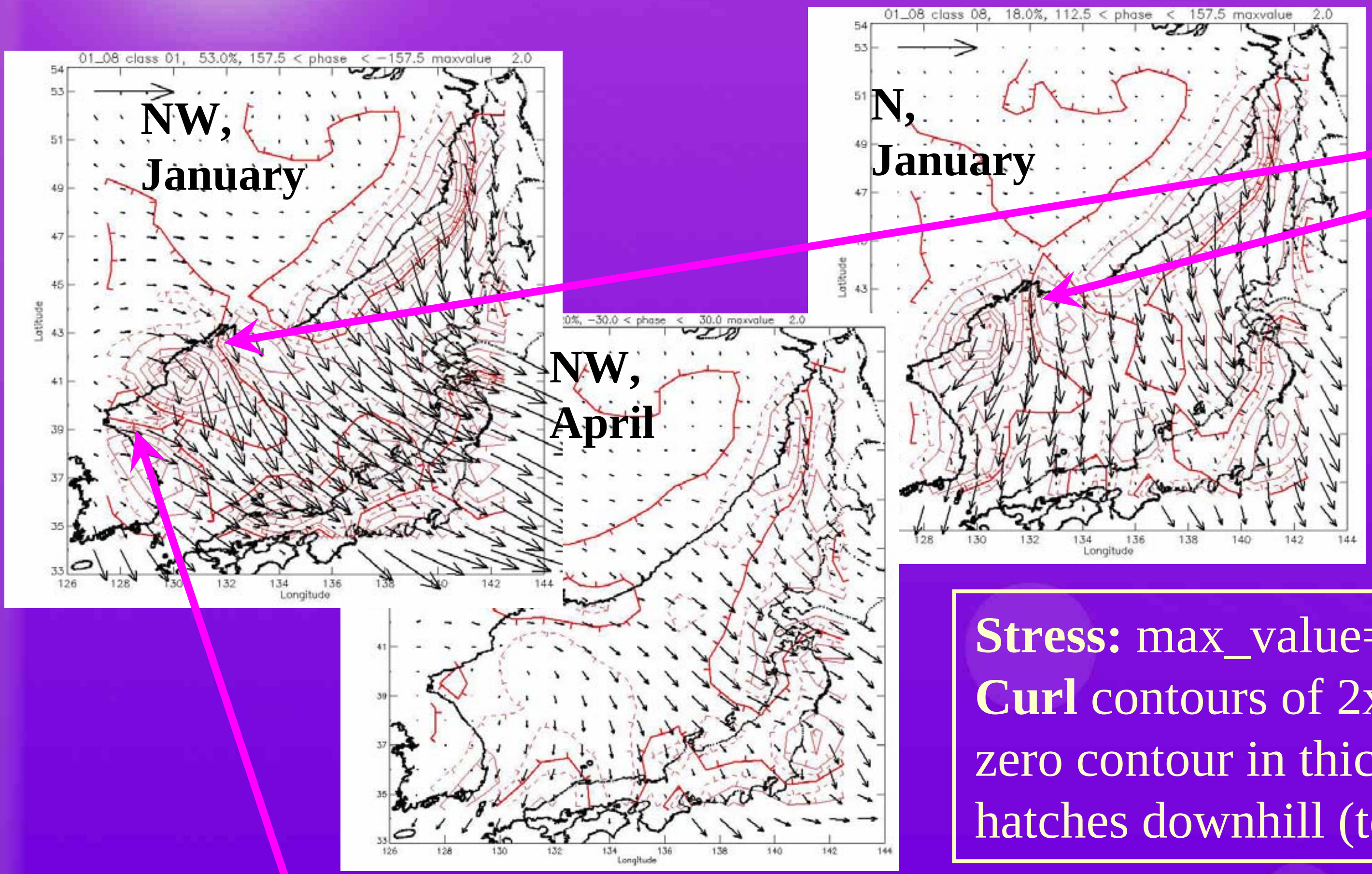

Stress curl dipole off Vladivostok (Kawamura and Wu, 1998; Dashko and Varlamov, 2000)

Stress: max_value=2 dyne/cm^2
Curl contours of 2x10^{-8} dyne/cm^3
zero contour in thick lines
hatches downhill (towards AC curl)

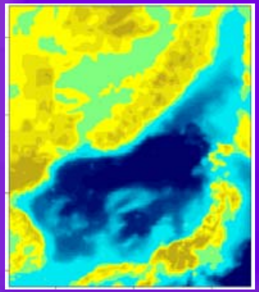

Cyclonic curl off East Korea Bay

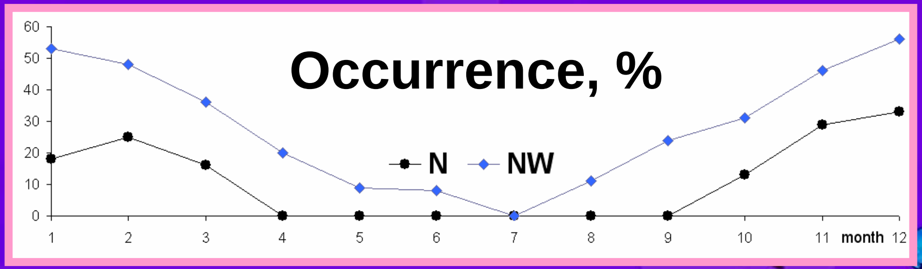

Western (W) pattern

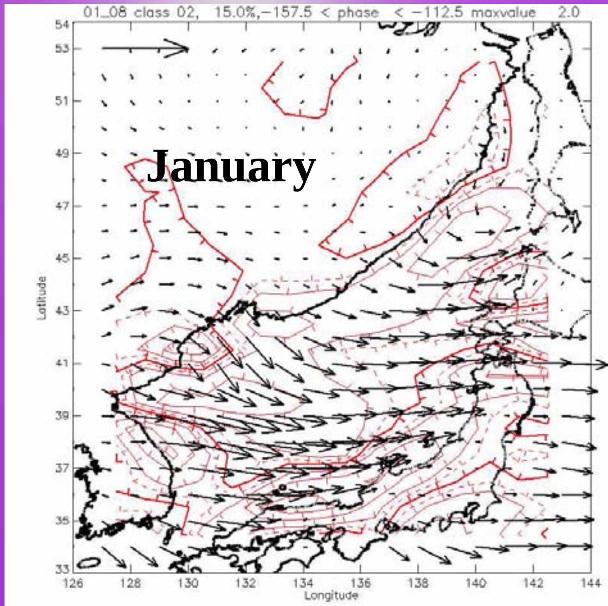

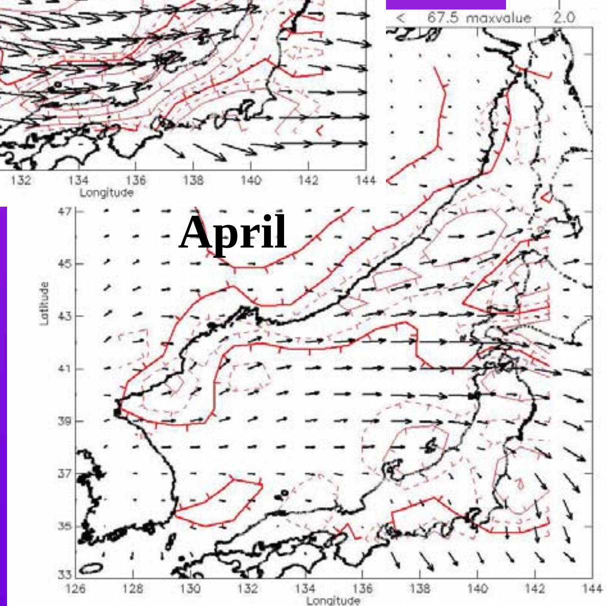

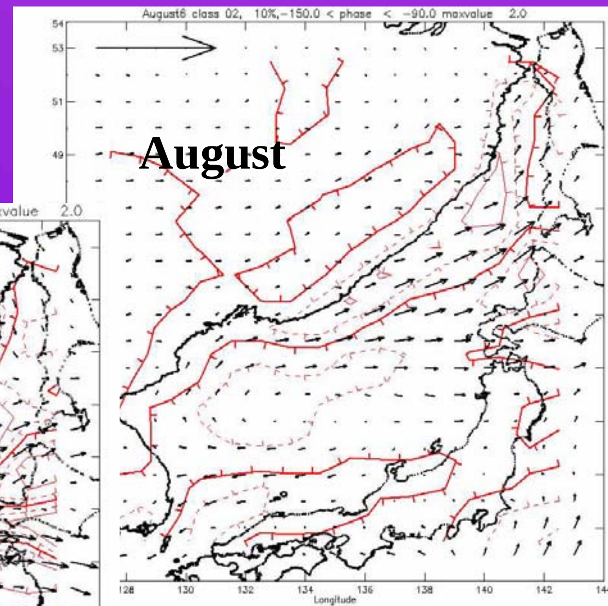

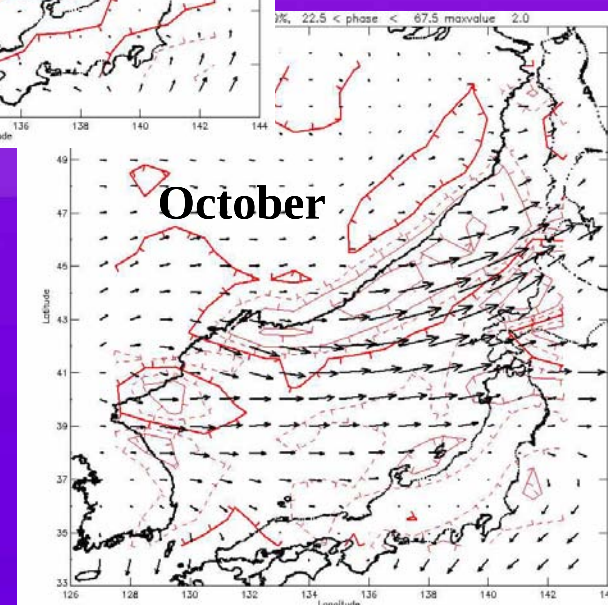

Stress: dyne/cm^2
Curl contours of 2×10^{-8} dyne/cm^3
Thick zero contour hatches downhill (towards AC curl)

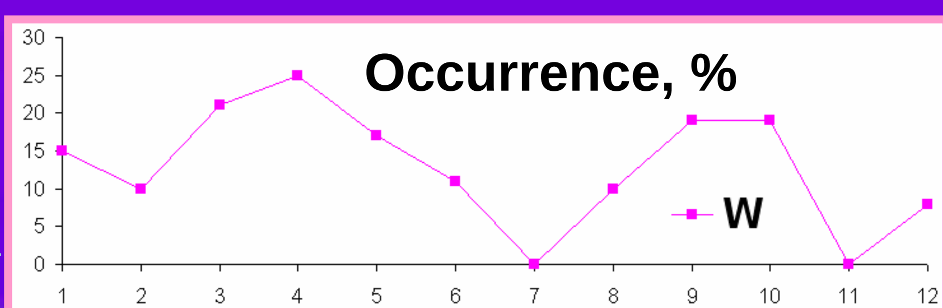

Southwest (SW) pattern

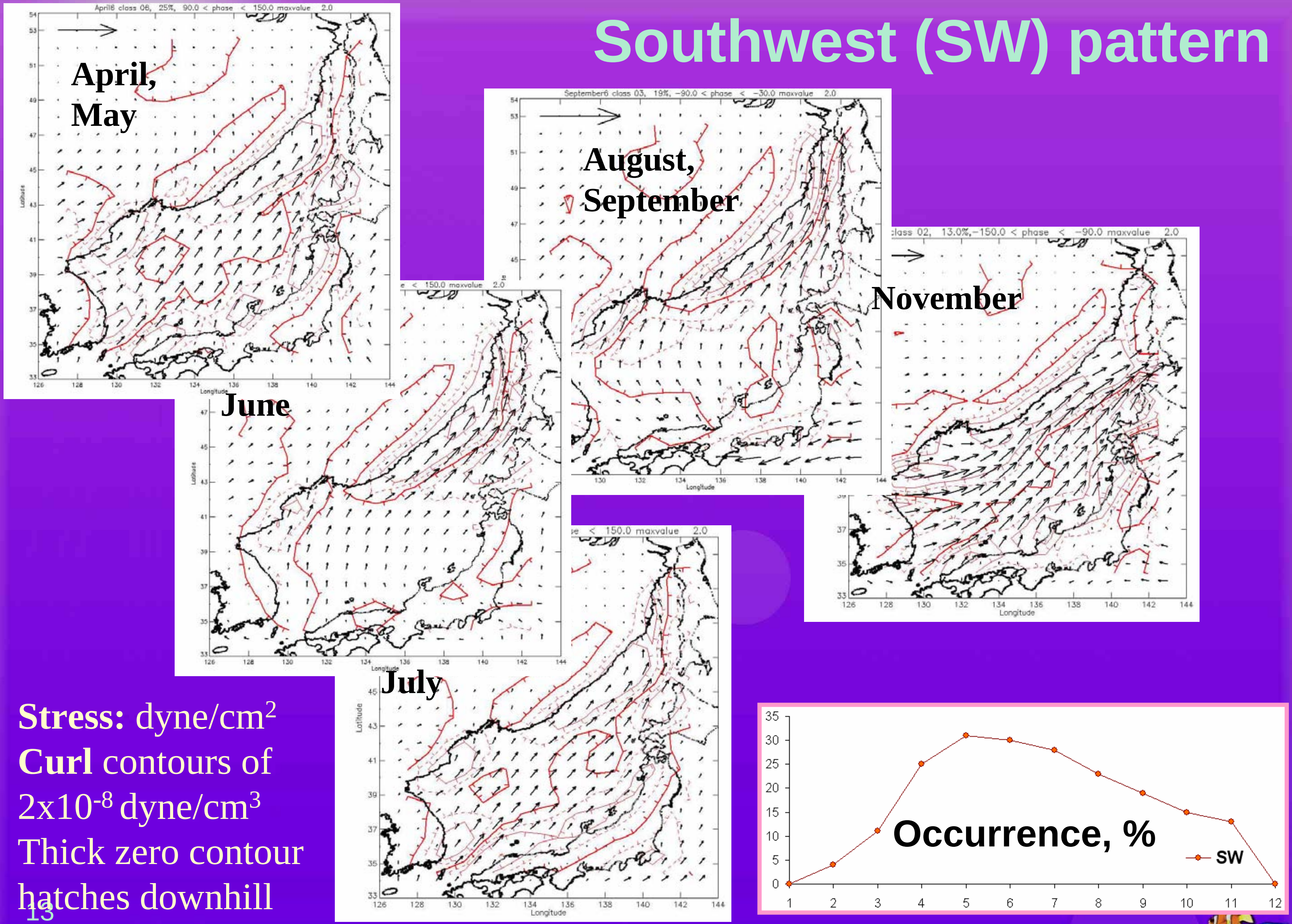

Stress: dyne/cm^2
Curl contours of
2×10^{-8} dyne/cm^3
Thick zero contour
hatches downhill
(towards AC curl)

South-southeast (S-SE) pattern

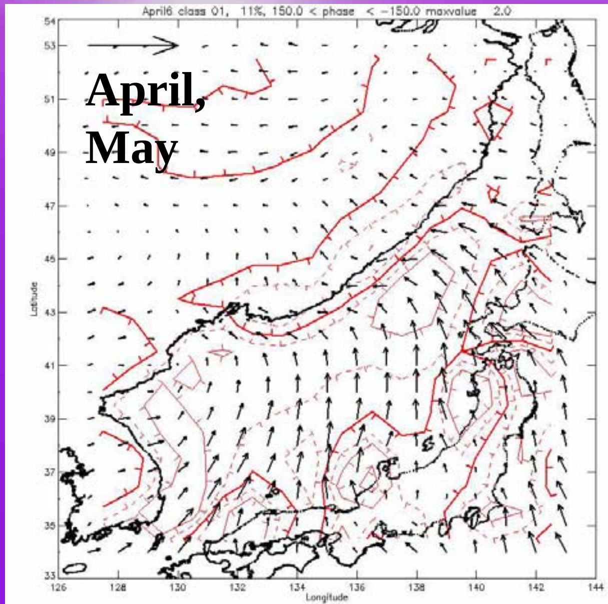

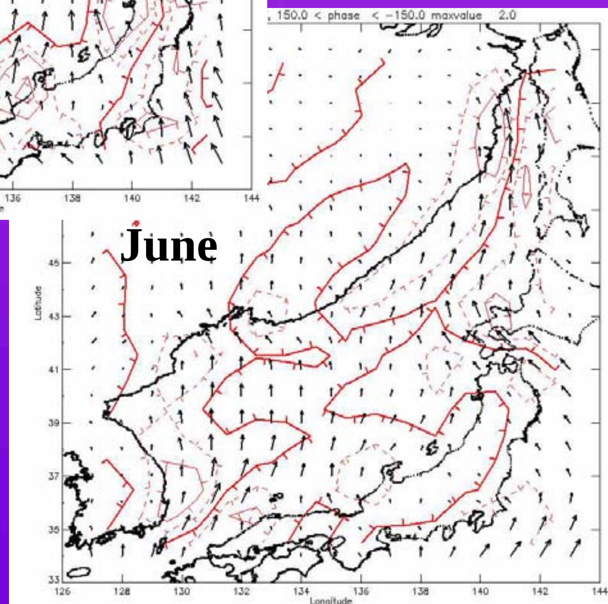

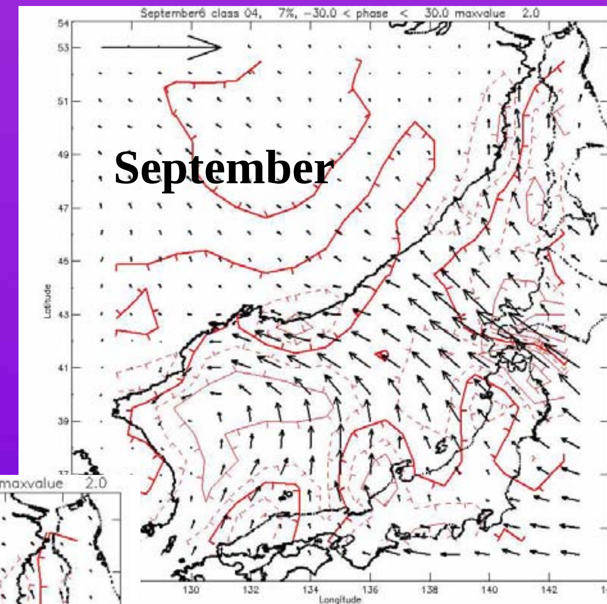

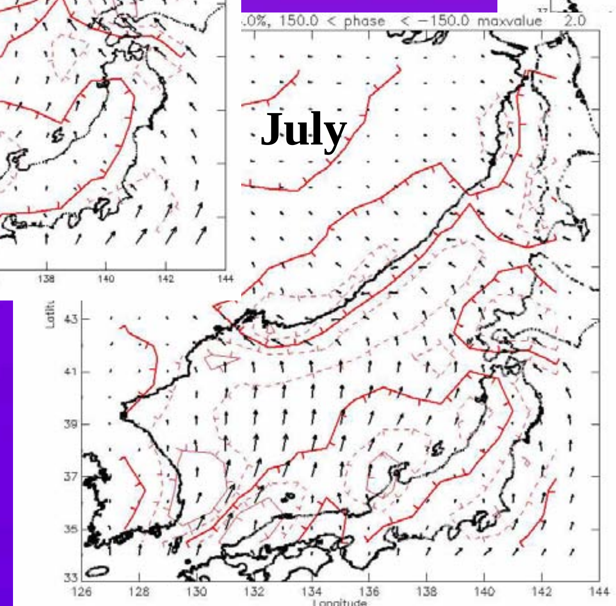

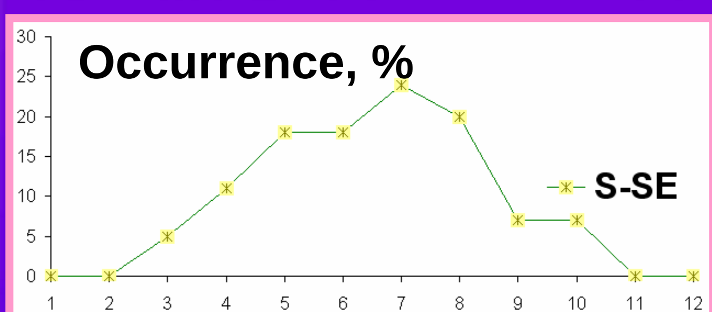

Stress: dyne/cm^2

Curl contours of 2×10^{-8} dyne/cm^3

Thick zero contour hatches downhill (towards AC curl)

East (E) and northeast (NE) patterns

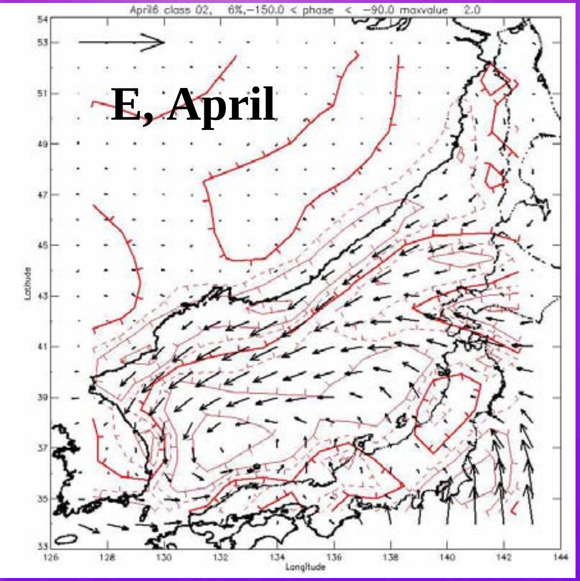

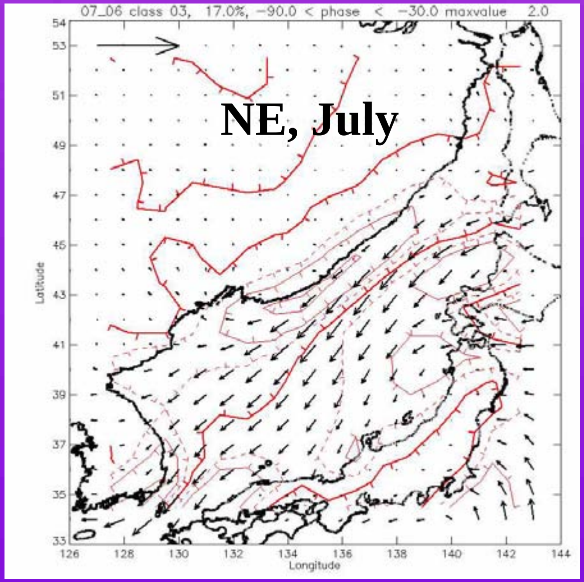

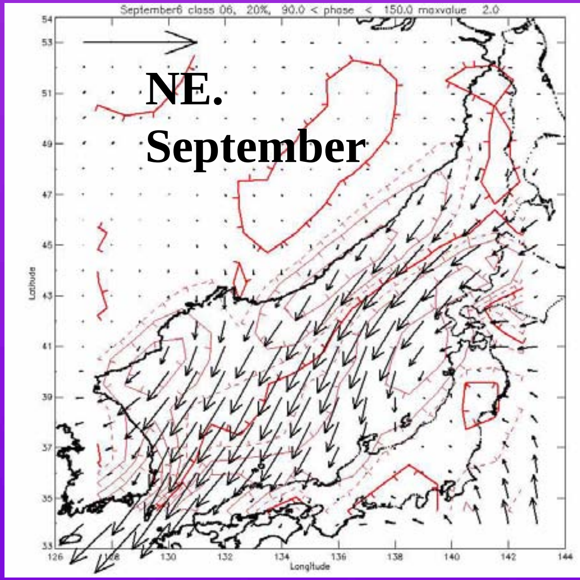

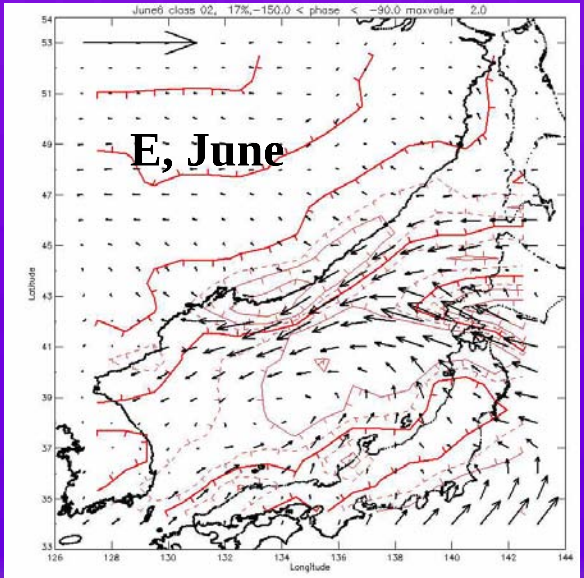

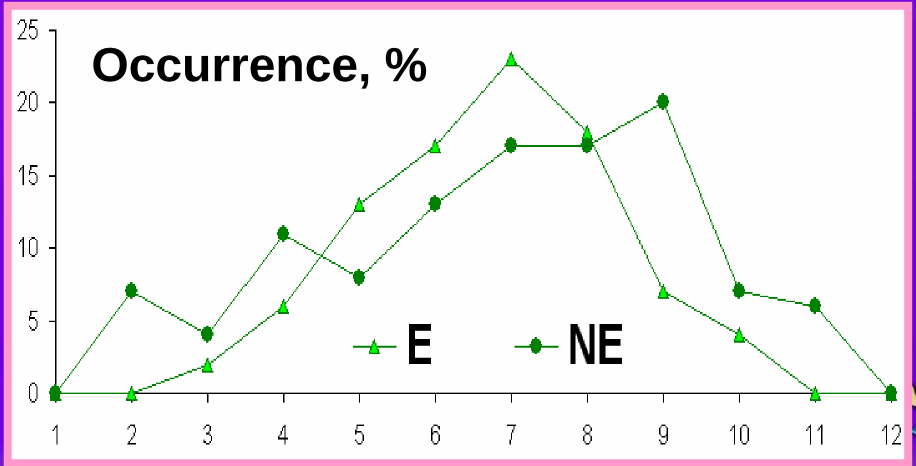

Monthly frequency of occurrence (%)
(for the whole period)

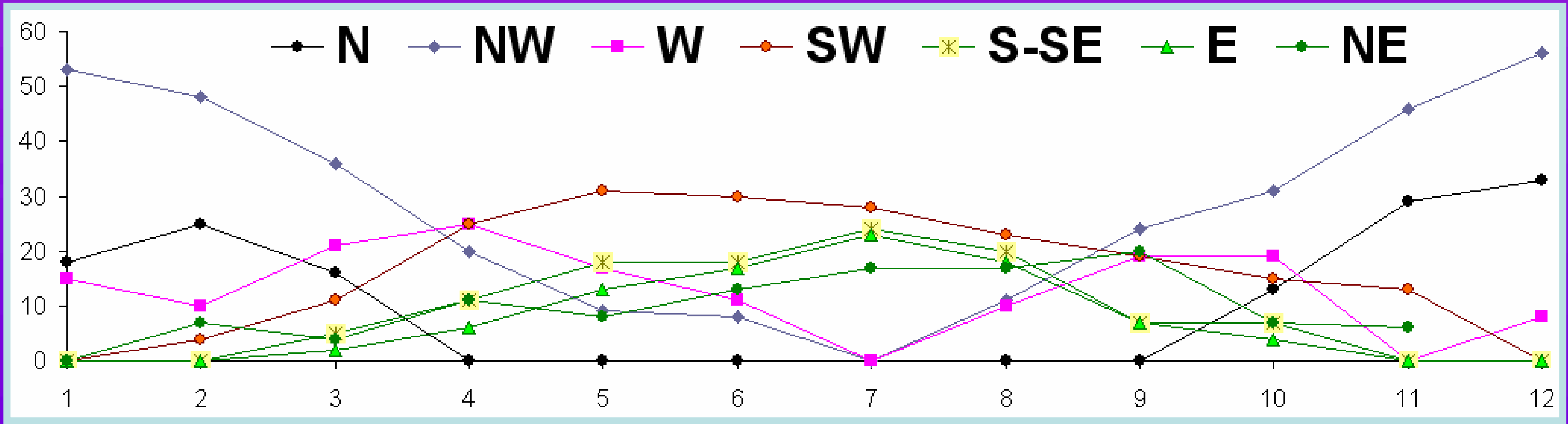

MHI oceanic model (Shapiro and Mikhaylova, 1992-1998)

JES model bathymetry

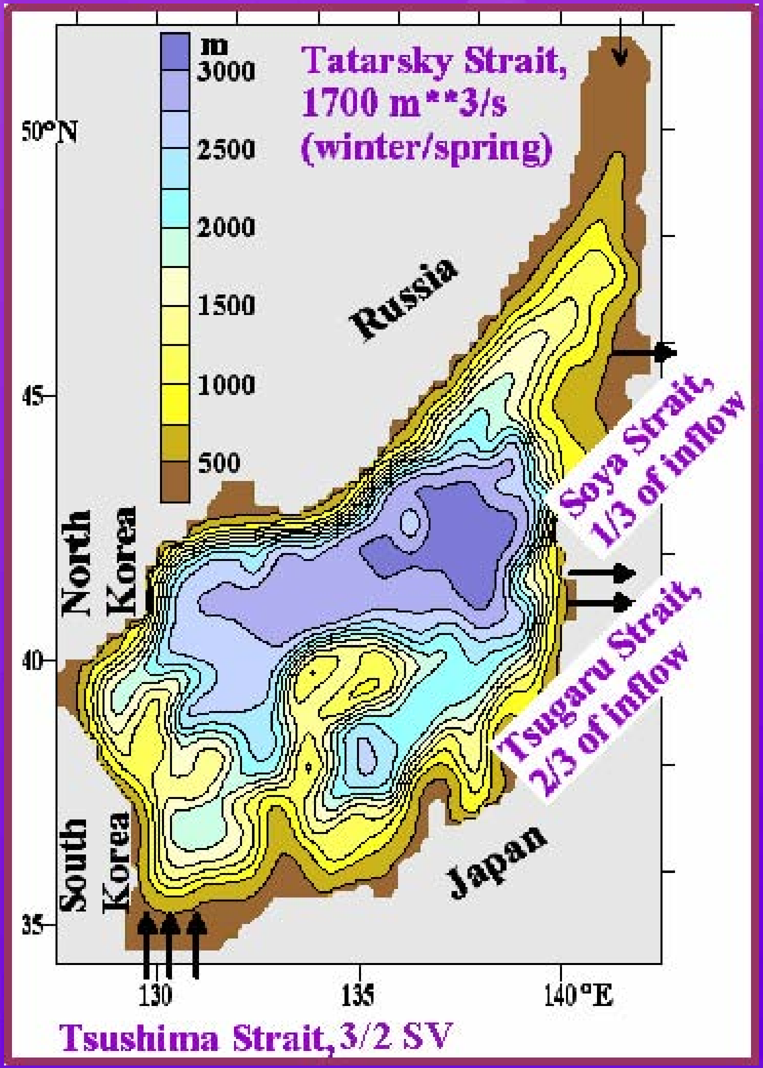

- 3D primitive equaion, quasi-isopycnic
- Lateral mesh of 1/8° (10-14 km)
- Surface buoyancy forcing for 1979-2001
- Inflow in the Korean Strait of 2-3 SV
- Wind forcing by typical patterns

for the warm season:

Run 1: mostly cyclonic curl (S-SE pattern)

Run 2: C/AC curl (SW pattern)

Run 3: strong C curl (E, NE patterns)

Cyclonic gyres in August

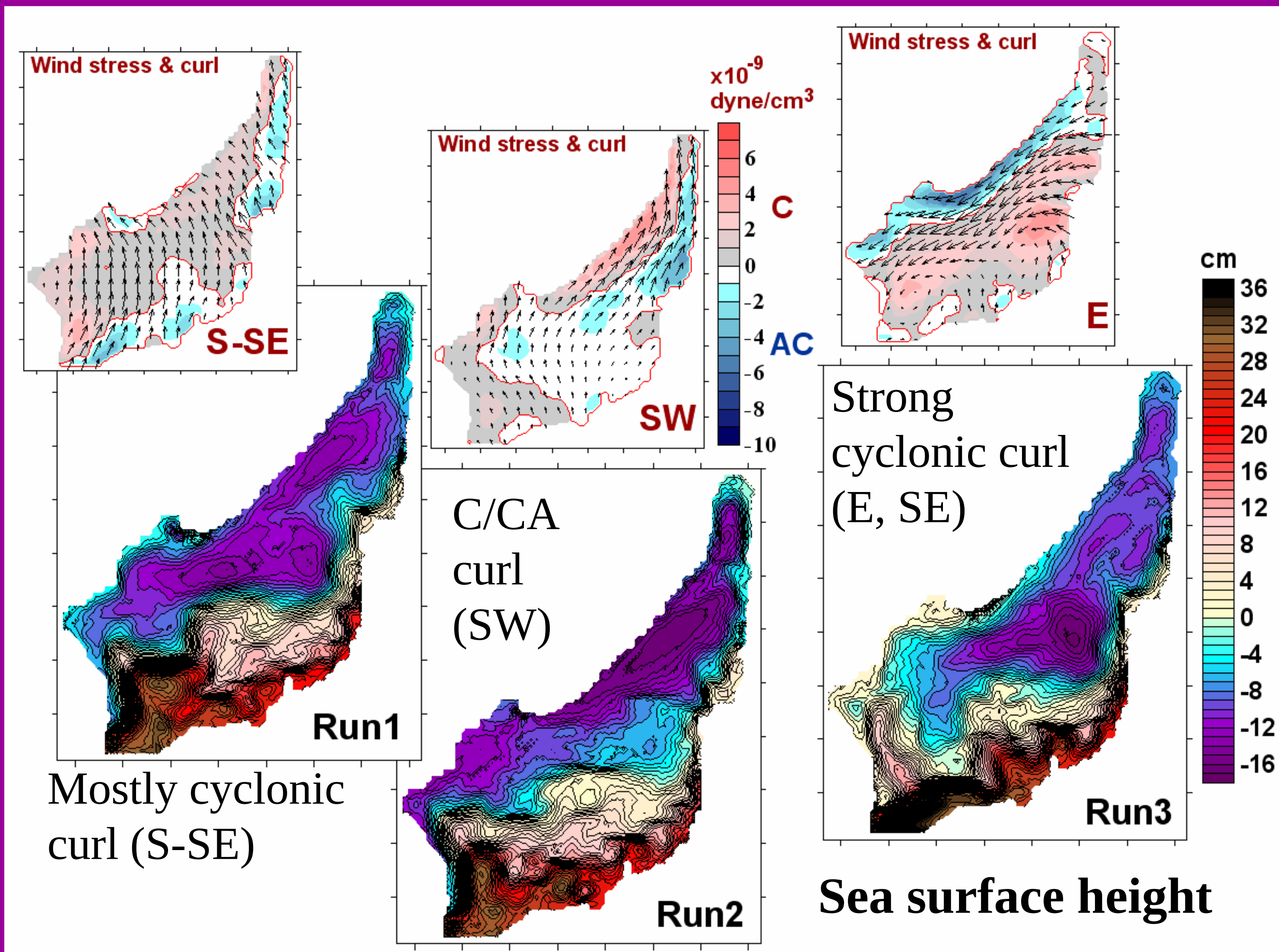

- Run 1: over the entire Japan Basin and Tatarsky Trough
- Run 2: in the NW JES and Tatarsky Strait
- Run 3: over the eastern Japan Basin

Effect of wind stress curl on branching of the Tsushima Current

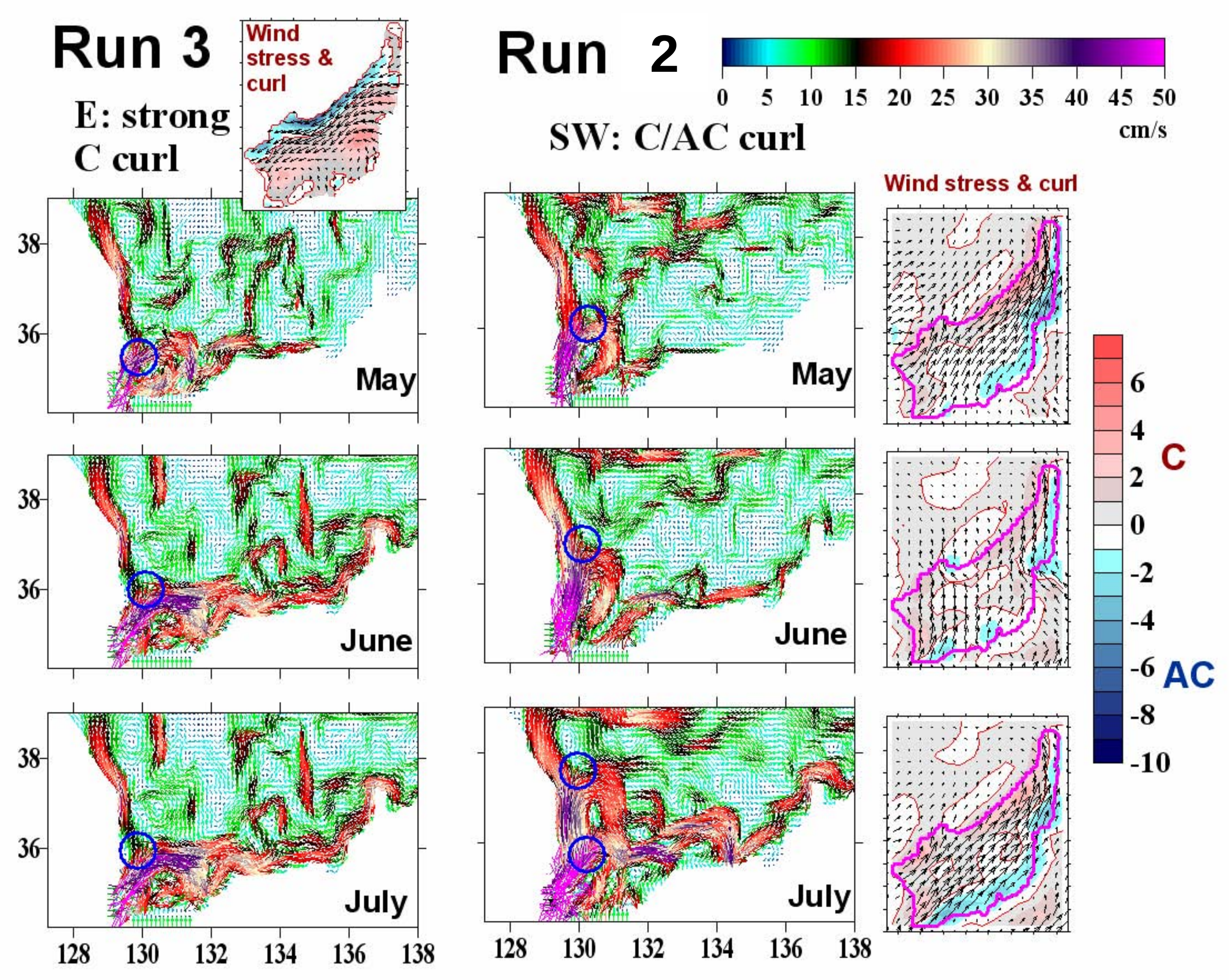

C vs. AC wind stress curl

(in the warm months)

- C_curl_most_JES
- C_curl_west_JES
- C_curl_east_JES
- AC_curl_most_JES
- AC_curl_west_JES
- AC_curl_east_JES

Occurrence, %

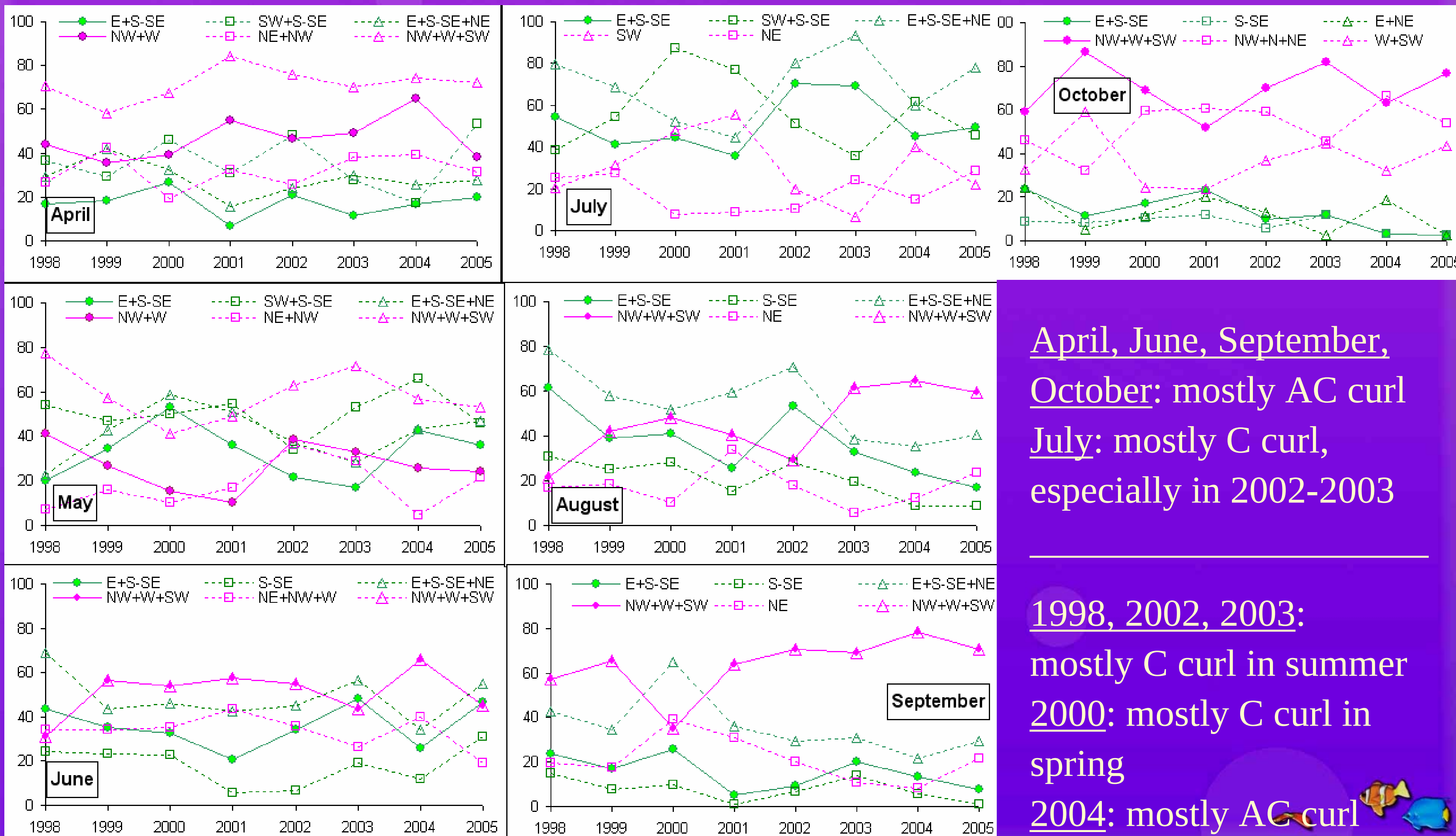

<u>April, June, September, October</u>: mostly AC curl

<u>July</u>: mostly C curl, especially in 2002-2003

<u>1998, 2002, 2003</u>: mostly C curl in summer

<u>2000</u>: mostly C curl in spring

<u>2004</u>: mostly AC curl

Conclusion

- Three major variability modes are revealed, associated with the prevailing wind direction typical for winter or summer monsoon (1), its zonal and meridional modulation (2), and cyclonic or anticyclonic vortex component (3).
- Wind stress and curl for typical patterns, derived from CEOF1 attributed to the prevailing wind direction, is strong both in the winter and summer monsoon.
- In the summer monsoon, patterns with cyclonic or anticyclonic curl over the JES are obtained, with their occurrence revealing considerable month-to-month and year-to-year variations.
- Wind patterns obtained have a distinctive effect upon the JES circulation